JOURNAL OF VIROLOGY, Sept. 2004, p. 9474–9486 Vol. 78, No. 17
0022-538X/04/$08.00+0 DOI: 10.1128/JVI.78.17.9474–9486.2004

Host Cell Specificity of Minute Virus of Mice in the Developing Mouse Embryo

Refael Itah,[1] Jacov Tal,[2] and Claytus Davis[1]*

Departments of Developmental Molecular Genetics[1] and Virology,[2] Faculty of Health Sciences, Ben-Gurion University of the Negev, Beer Sheva, Israel

Received 23 October 2003/Accepted 1 April 2004

Productive infection by the murine autonomous parvovirus minute virus of mice (MVM) depends on a dividing cell population and its differentiation state. We have extended the in vivo analysis of the MVM host cell type range into the developing embryo by in utero inoculation followed by further gestation. The fibrotropic p strain (MVMp) and the lymphotropic i strain (MVMi) did not productively infect the early mouse embryo but were able to infect overlapping sets of cell types in the mid- or late-gestation embryo. Both MVMp and MVMi infected developing bone primordia, notochord, central nervous system, and dorsal root ganglia. MVMp exhibited extensive infection in fibroblasts, in the epithelia of lung and developing nose, and, to a lesser extent, in the gut. MVMi also infected endothelium. The data indicated that the host ranges of the two MVM strains consist of overlapping sets of cell types that are broader than previously known from neonate and in vitro infection experiments. The correlation between MVM host cell types and the cell types that activate the transgenic P4 promoter is consistent with the hypothesis that activation of the incoming viral P4 promoter by the host cell is one of the host range determinants of MVM.

The autonomously replicating parvoviruses are small, nonenveloped, icosahedral DNA viruses of vertebrates. They include several economically important livestock viruses and the human-specific member B19, which causes erythema infectiosum, a common childhood disease. Phylogenetic analysis (23) suggests the existence of two major branches of the mammalian autonomous parvoviruses, with the bovine, chipmunk, and primate viruses in one lineage and the carnivore, pig, and other rodent viruses in the other. Minute virus of mice (MVM), the best studied of the rodent parvoviruses (18), contains a 5,149-nucleotide single-stranded genome. The viral genome harbors two transcription units encoding two nonstructural (NS) and three structural (VP) proteins. Almost all aspects of the viral life cycle are dependent upon virus-host interactions, and MVM has proven to be an excellent model system for studying these. Upon infection of a permissive host, the single-stranded viral genome is converted to a double-stranded replicative-form DNA, following which the viral nonstructural promoter, P4, is activated by the host (11), leading to the synthesis of the nonstructural NS1 and NS2 proteins. Host and viral functions cooperate in the subsequent amplification and expression of the viral genome.

Whether a potential host cell is permissive has been shown to depend on a number of cellular characteristics. In vitro experiments indicate an absolute requirement for a dividing cell population and S-phase functions (36, 43). MVM infection also depends upon the degree of differentiation of the host cell in vitro (16, 37) and in vivo (4, 9). However, the nature of this dependency has not been elucidated; several tissues in the adult animal that contain actively dividing cells are not targets for parvovirus replication. Study of two MVM strains, the fibrotropic p strain (MVMp) (8, 36) and the lymphotropic i strain (MVMi) (25), indicate a cell type-dependent interaction between the host and the virus capsid proteins. The two strains exhibit 97% sequence identity and are serologically indistinguishable, yet they differ radically in their tropisms in vitro, displaying reciprocal cell type specificities. MVMp establishes productive infection in cultured mouse fibroblasts, whereas MVMi replicates lytically in mouse T lymphocytes (3). Growth of each is restricted in the other's permissive cell types (16, 38). Entrance of MVMi and MVMp particles into the host cell is mediated by the same cell surface receptor (34), which was found in abundance on mouse permissive A9 cells (22). The host range variation is determined intracellularly by a capsid determinant consisting of a limited number of amino acids in VP2 (1, 24) and which is assumed to interact with a still-unknown host factor. Other than the VP2-host interaction, Rubio et al. have demonstrated cell-type-dependent interactions between host cellular factors and the NS proteins (33). Activation of the viral P4 promoter by the host following infection is a critical early step in the viral life cycle (11) and is completely dependent on the host transcription machinery. Since promoter activities often vary widely in different cell types and at different developmental stages, it is possible that the initial activation of P4 in the completed double-stranded viral genome constitutes a host range determinant. Indeed, we have recently shown that host activation of a transgenic P4 promoter is tissue and developmental stage specific and loosely correlates with tissue type susceptibility to MVM (9). Finally, NS2 was shown to be essential for productive infection in a cell-type-specific fashion in vitro (6) and in vivo (5).

Infection studies with live animals have shown that the two MVM strains differ in their pathogenicities. Infection of adult or neonatal mice with MVMp was asymptomatic (5, 21). Analyses of viral distribution revealed significant amounts of MVMp in the gastrointestinal tract, frequently in fibroblasts

* Corresponding author. Mailing address: Department of Developmental Molecular Genetics, Faculty of Health Sciences, Ben-Gurion University of the Negev, Beer Sheva, Israel. Phone: 972 8 647 9956. Fax: 972 8 627 6215. E-mail: clay@bgumail.bgu.ac.il.

(5). In contrast, MVMi infection in neonates was lethal, probably due to its affinity for the capillary endothelium of the renal medulla, cells which MVMp fails to infect (4). MVMi was shown to be able to infect still-dividing neuroepithelial cells in the neonate brain (31). Other mammalian parvoviruses have varied tropisms in vivo (17, 41), with an overall tropism for the hematopoetic/lymphoid tissues, gut, heart, and proliferative neuroepithelium (13, 29).

Despite the dependence on a dividing cell population and sensitivity to differentiation status, MVM infection has rarely been studied in the developing embryo, which consists largely of dividing cells in a wide range of differentiation states. Early studies showed that some rodent parvoviruses could induce fetal disease in laboratory animals. Following maternal injection, transplacental infection of mid-gestation rat embryos with parvovirus occasionally took place (20, 40), resulting in mongoloid deformities, craniofacial lesions, and microcephaly (39), without observable effect on the mother. In embryonic tissues, parvovirus H1 inclusions were identified in developing bone, the basal layer of the dermis, the muscular and lamina propria layers of the gastrointestinal tract, tooth germ, and vascular endothelium. Early-gestation embryos were resistant to infection (40). At least the bovine, porcine, and canine parvoviruses have also been shown to cause transplacental infection of gestating embryos, infecting, in the pig, the fetal myocardium and lung (2, 26).

In this study we report the susceptibilities of different mouse embryonic cell types to MVMi and MVMp infection following in utero injection of MVM and further gestation. We compare these to the published cell type tropisms of the two viral strains and to the distribution of embryonic activation of a transgenic MVM P4 promoter.

MATERIALS AND METHODS

Virus preparation. MVMp and MVMi stocks were grown in suspension in A9 (peritoneal tumor-derived Ehrlich ascites) and EL4 (mouse lymphoma) cells and purified by CsCl or glycerol gradient centrifugation, and titers were determined by plaque assay in NB324K indicator cells as described previously (32).

Mouse care. Hsd:ICR mice, a locally maintained (Harlan, Rehovot, Israel) population of the outbred strain CD-1, were kept in the medical faculty animal care facility. All housing and experimental procedures followed institution-approved protocols and guidelines. Females fed a high-fat (8%) breeder diet were mated to males and were checked the following morning for vaginal plugs. The morning on which a vaginal plug was observed was considered to be 0.5 day postconception (dpc). Females were housed individually throughout pregnancy and experimentation.

Surgical procedure. Virus was injected at 9.5 or 12.5 dpc as described previously (17a). After abdominal incision, the number of embryos on each uterine horn was recorded. At 9.5 dpc, the embryo itself is not visible through the uterine wall and the embryonic organ primordia are very small; therefore, 2 μl of inoculum containing 10^5 PFU of MVM was injected into the amniotic cavity. Four microliters of inoculum was injected into the livers of 12.5-dpc embryos. No more than four embryos, all on one uterine horn, were injected. Following 24, 48, or 96 h of further gestation, the females were killed by cervical dislocation. The abdominal wall was opened, and the injected embryos and at least two contralateral uninjected control embryos were taken for analysis. Any resorption sites or dead embryos were noted.

Histology and immunohistochemistry. Only living, morphologically and histologically normal embryos were chosen for histological analysis. Once triggered, embryonic resorption is morphologically distinguishable within a few hours, which is less than the life cycle of MVM. The observed MVM immunoreactivity is due to infection of normal, not resorbing, embryos.

Injected and control embryos were embedded in OCT (TissueTek) and frozen by immersion into liquid nitrogen. Individual frozen embryos were serially sectioned at 16 μm in a cryomicrotome (IEC) and collected on poly-L-lysine coated slides. Air-dried sections were fixed for 10 min in 4% paraformaldehyde and rinsed four times in Tris-buffered saline (TBS) for 12 min. Sections were blocked with 1% bovine serum albumin (BSA) in TBS and then incubated for 1 h at room temperature with the primary antibody (polyclonal anti-MVM capsid protein purified from rabbit serum) diluted 1:500 in 1% BSA in TBS. The slides were then rinsed in TBS as after fixation and incubated for 1 h at room temperature with one of two equivalent, minimally mouse-cross-reactive secondary antibodies, Alexa Fluor 546-conjugated goat anti-rabbit immunoglobulin G heavy plus light chains (Molecular Probes) or Cy3-conjugated affinity-pure goat anti-rabbit immunoglobulin G heavy plus light chains (Jackson ImmunoResearch), diluted 1:250 in 1% BSA in TBS. Slides were then rinsed as before, and coverslips were applied in glycerol containing 1 mg of phenyldiamine per ml. Immunoreactivity or tissue was visualized on a Leica DMR compound microscope equipped for immunofluorescence and differential interference contrast (DIC) and photographed with a Spot RT digital camera (Diagnostic Instruments).

RESULTS

The injection procedure developed has been described in detail (17a) and was demonstrated to be effective and benign. Injection of sterile saline at either embryonic stage did not significantly perturb embryonic development. The efficacy was confirmed either by observing the healing needle wound in the injected embryonic liver after 24 h of further gestation or by injecting India ink into 9.5-dpc yolk sacs, dissecting immediately after, and observing the distribution of the ink. We therefore used the procedure to characterize the pattern and kinetics of MVM infection in the developing mouse embryo. The times of injection and analysis relative to the activity of a transgenic MVM P4 promoter at different developmental stages are illustrated in Fig. 1.

MVMi is more pathogenic than MVMp. The relative pathogenicities of MVMi and MVMp in mouse embryos were assessed following intrauterine inoculation. Two microliters of MVMi or MVMp (10^5 PFU) was injected into the amniotic sacs of 9.5-dpc embryos. Four microliters was injected into embryonic livers of 12.5-dpc embryos as described in Materials and Methods. Gestation was left to proceed for an additional 24, 48, or 96 h. The patterns of surviving embryos and resorption sites were scored (Table 1). MVMi injection at 12.5 dpc was significantly more likely to result in embryonic death than MVMp injection ($P_{\text{null}} < 0.01$) over the times shown. Injection did not result in any significant increase in resorption among contralateral or uninjected adjacent embryos. To examine whether the greater survival of MVMp injected embryos indicated a recovery from infection or a slower pathology, 20 embryos in five females were injected and the pregnancies were left to continue for 120 h, i.e., within 2 days of parturition. The females were then killed, and the patterns of embryos and resorption sites on the uterine horns were determined. By this late stage, 17 of the 20 injected embryos had resorbed, suggesting that MVMp may ultimately be as lethal as MVMi but takes longer to kill the host embryo.

Distribution of infection. Injected embryos, uninjected neighboring embryos, and contralateral uninjected control embryos were removed and cryosectioned. The distribution of MVM capsid proteins in different tissues and cell types was determined by immunohistochemistry.

At 9.5 dpc, 13 embryos were injected with MVMp or MVMi. After 48 h of further gestation, we observed resorption of five embryos and retarded development of one. There was no significant difference between MVMp and MVMi. Five MVMp-

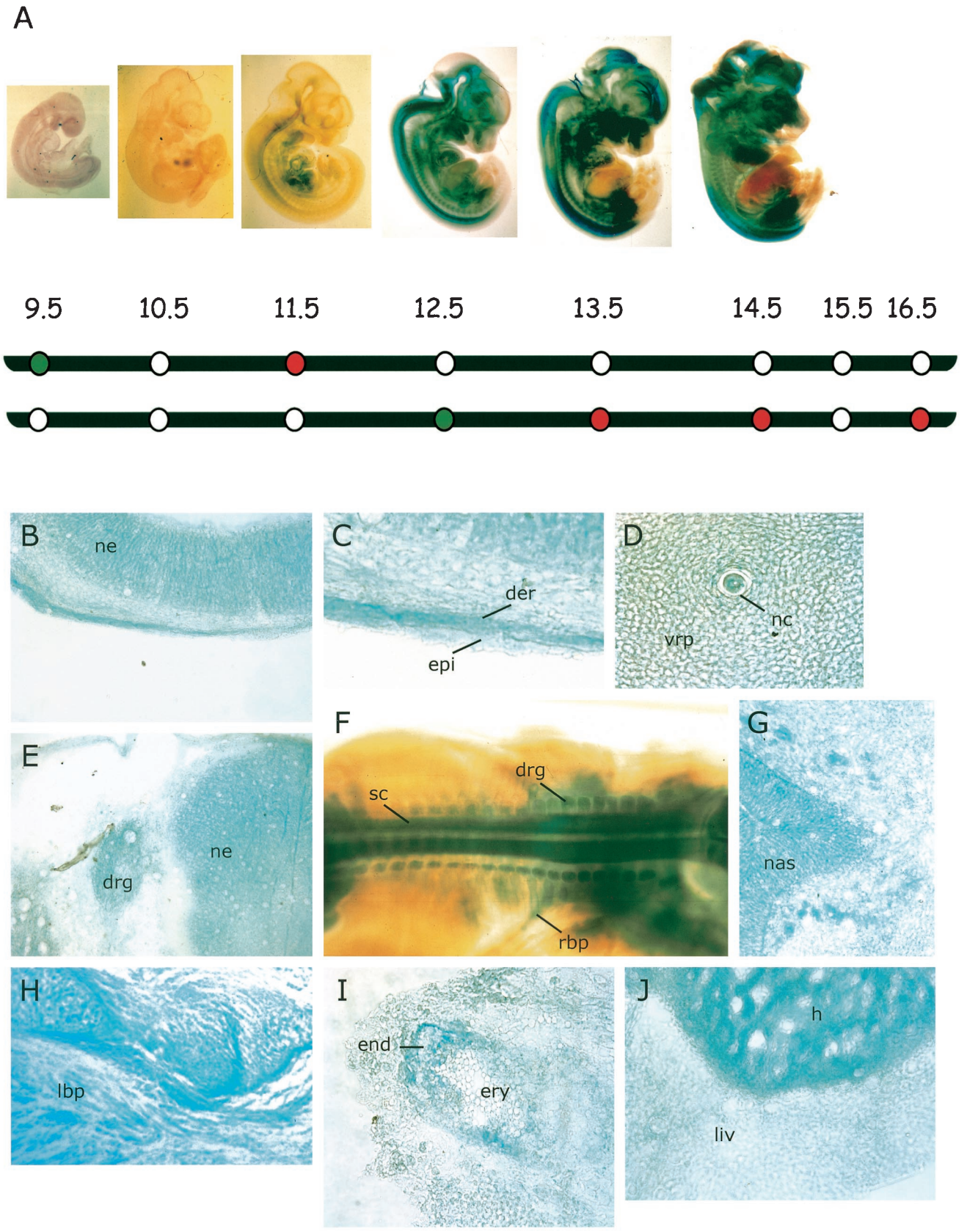

FIG. 1. MVM injection and analysis relative to activity of a transgenic MVM P4 promoter. (A) Gestation series showing activity of a transgenic MVM P4 promoter visualized by β-galactosidase reporter activity (blue) at the indicated times (dpc). Green dots indicate inoculation with MVM;

TABLE 1. Embryo fatality following MVMp/ or MVMi injection[a]

Virus	Injection time (dpc)	Embryo death at:								
		24 h			48 h			96 h		
		No. of embryos injected	No. of resorptions	% Resorbed[b]	No. of embryos injected	No. of resorptions	% Resorbed[b]	No. of embryos injected	No. of resorptions	% Resorbed[b]
MVMp	9.5	ND[c]	ND		8	3	40	ND	ND	
MVMi	9.5	ND	ND		5	2	40	ND	ND	
MVMp	12.5	7	2	30	10	4	40	12	4	30
MVMi	12.5	6	4	70	15	10	70	20	12	60

[a] MVMi and MVMp were injected into 9.5- or 12.5-dpc mouse embryos as described in Materials and Methods. After 24, 48, or 96 h of incubation, the extent of embro death was assessed by counting the number of resorption sites among the the injected embryos.
[b] Rounded to nearest 10%.
[c] ND, not determined.

and three MVMi-injected embryos and their placentas were removed and sectioned, and the distribution of MVM coat proteins was determined by immunohistochemistry. A widespread but diffuse and weak increase in signal compared to uninjected control samples was apparent in all tissues of embryos injected with either virus strain. The signal was stronger in the central nervous systems (CNS), the dorsal aortas, and the hearts of MVMp-inoculated embryos (Fig. 2) and was stronger in the CNS of MVMi-inoculated embryos. In contrast to the results for the embryos, the developing placentas exhibited a much stronger virus coat protein signal distributed in regional foci on only the embryonic side of the placenta, with increased signal observed around blood vessels (Fig. 2C and D). Since the placenta itself was not injected, the route of infection must have been through either the amniotic fluid or, more likely, embryonic blood circulation to the placenta.

By 12.5 dpc embryonic organogenesis is well under way, and a greater variety of more fully differentiated cell types are found in the embryo than at 9.5 dpc. By this stage the transgenic MVM P4 promoter was active in a wide variety of different cell types (9) (Fig. 1). We therefore examined the course and extent of MVM infection in the developing embryos by injecting the virus directly into the embryonic livers of 12.5-dpc embryos and examining the distribution of MVM coat proteins after a further 24, 48, or 96 h of gestation following inoculation.

At 24 h following inoculation, 7 embryos out of 13 injected embryos from three females were serially sectioned and stained for MVM viral capsid proteins. The wound due to the injection into the liver was clearly visible and showed intense local immunoreactivity (not shown). Outside the injection site itself, liver tissue was completely negative for viral capsid proteins in both MVMp- and MVMi-injected embryos. In the rest of the embryo, localized staining was observed only in small patches in chondrocytes of some bone primordia and in the notochord (Fig. 3B and C).

At 48 h after inoculation, the initial weak and patchy staining observed in bone primordia became somewhat more extensive and intense (Fig. 3F, H, I, and J). The bone primordium staining was restricted to the developing axial skeletal elements, the limb and mandibular bones of the head. Each of the infected cells showed punctate signal distributed mainly in the cytoplasm. No staining was observed in any other tissues, including the area where the flat bones of the skull will form.

The infection pattern seen after 96 h of gestation following inoculation was much more extensive than that observed at shorter incubation times. Individual positive cells were observed scattered throughout the dorsal root ganglia of both MVMp- and MVMi-inoculated embryos (Fig. 4C and E), although positive cells in the MVMp-inoculated embryos were more likely to be found at the periphery of the dorsal root ganglia. Similarly, scattered positive cells were observed in the developing CNS of both MVMp- and MVMi-inoculated embryos (Fig. 4F, G, and I). Positive cells were more frequently observed in the CNS of MVMi-inoculated embryos, in which immunoreactivity appeared more frequently near the interface between the actively dividing cells of the ventricular zone and the overlying marginal zone, which contains the postmitotic neurons (Fig. 4F).

By 96 h, aspects of MVM strain tropisms were apparent in the patterns of embryonic infection. MVMi infection was found in the endothelia of some blood vessels (Fig. 5C), notably in the liver, lung, spleen, dermis, and branch vessels in bone, and in a few scattered cells that were judged to be lymphocytes on the basis of morphology (not shown). We never observed signal in the endothelia of MVMp-inoculated embryos. However, extensive and intense MVMp staining was observed in fibroblastic tissues throughout the embryo, including the dermis (Fig. 6B), connective tissues (Fig. 6D), head mesenchyme (Fig. 5J), developing bone periost (Fig. 6F), heart (Fig. 6H and I), and lung epithelium (Fig. 5H), and to a lesser extent in the developing gut (data not shown). Both MVMp

red dots indicate stage at time of analysis. (B to J) Tissue-specific activity of a transgenic MVM P4 promoter, as visualized by β-galactosidase reporter activity at 12.5 or 13.5 dpc. (B) Forebrain neuroepithelium, mesenchyme, and skin. (C) Enlargement of skin region in panel B. (D) Section through vertebra primordium and notochord. (E) Section through spinal chord and dorsal root ganglion. (F) Dorsal view of 13.5-dpc whole-mount embryo, showing staining in CNS, developing bone primordium, and dorsal root ganglion. (G) Fold of nasal epithelium. (H) Section through developing limb bud. (I) Blood vessel. (J) Section through heart and liver. der, dermis; drg, dorsal root ganglion; end, endothelium; epi, epidermis; ery, erythrocytes; h, heart; lbp, limb bone primordium; liv, liver; nas, nasal epithelium; nc, notochord; ne, neuroepithelium; rbp, rib primordium; sc, spinal chord; vrp, vertebra primordium.

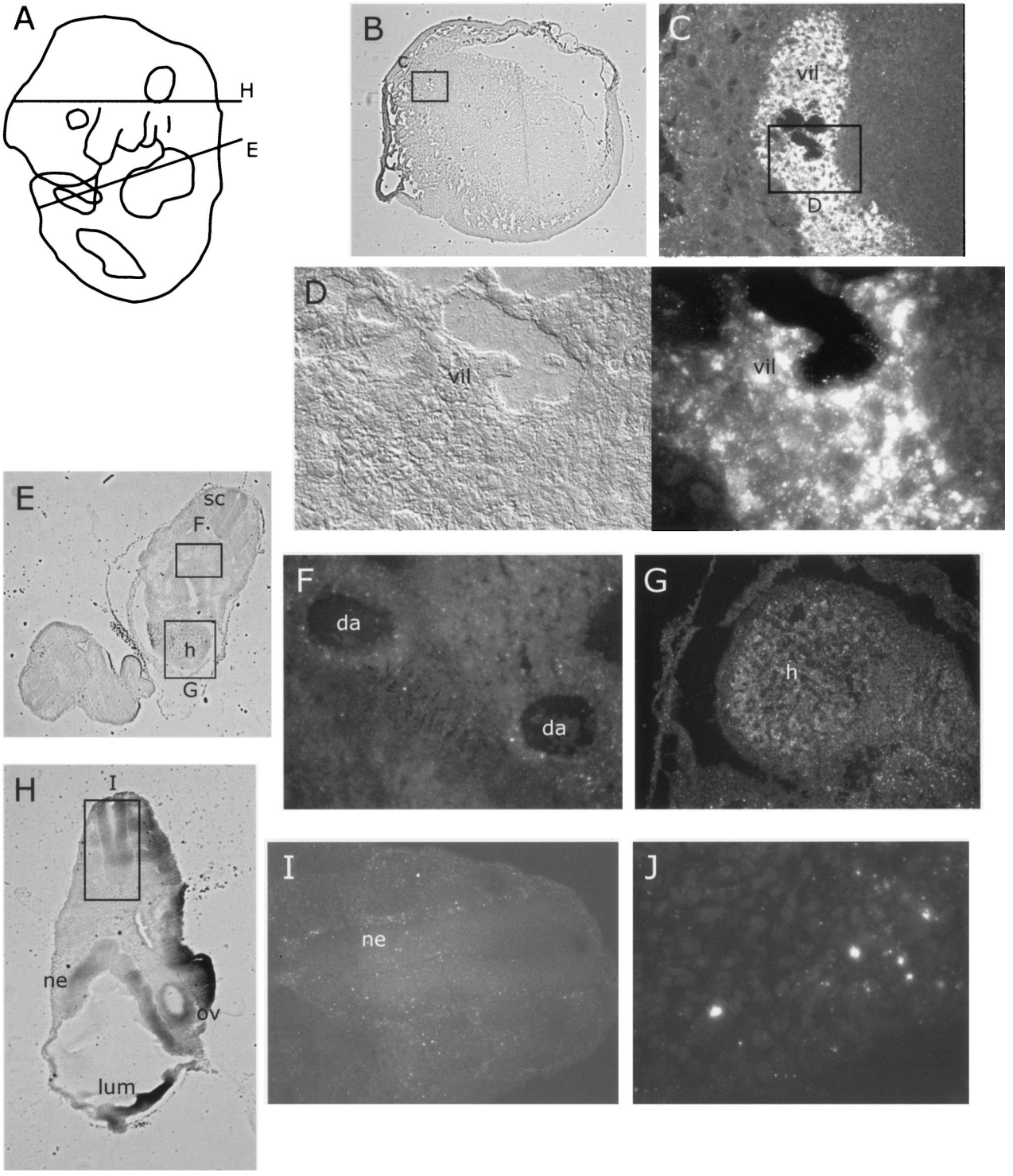

FIG. 2. MVM immunoreactivity following inoculation at 9.5 dpc and 48 h of further gestation. This and subsequent figures follow a similar format. Embryo diagrams (after reference 19) at the top left illustrate the embryonic stage and position of histological cuts in the figure elements. Low-magnification images of the entire embryo section are included on the left of the figure panels if available, and rectangular insets labeled with a capital letter at the top or bottom indicate the area covered by the corresponding figure element. Double images bearing a single-letter label are identical fields of view under different illuminations, with DIC on the left and immunofluorescence showing the distribution of MVM coat proteins on the right. (A) Diagram of 11.5-dpc embryo, showing section levels in panels E and H. (B) Section through an 11.5-dpc placenta associated with an MVMp-injected embryo. (C) Enlargement of region in panel B showing MVM infection in embryonic chorionic villus but not surrounding maternal tissue. (D) DIC (left) and immunofluorescence (right) detail of region of villus in panel C showing individual MVM-infected cells. (E to J) Sections through 11.5-dpc embryo (E and H) showing weak and scattered anti-MVM immunoreactivity in the dorsal aorta (F), heart (G), and neuroepithelium (I). (J) Detail of heart showing scattered punctate staining. da, dorsal aorta; h, heart; lum, CNS lumen; ne, neuroepithelium; ov, otic vesicle; sc, spinal chord; vil, placental villus.

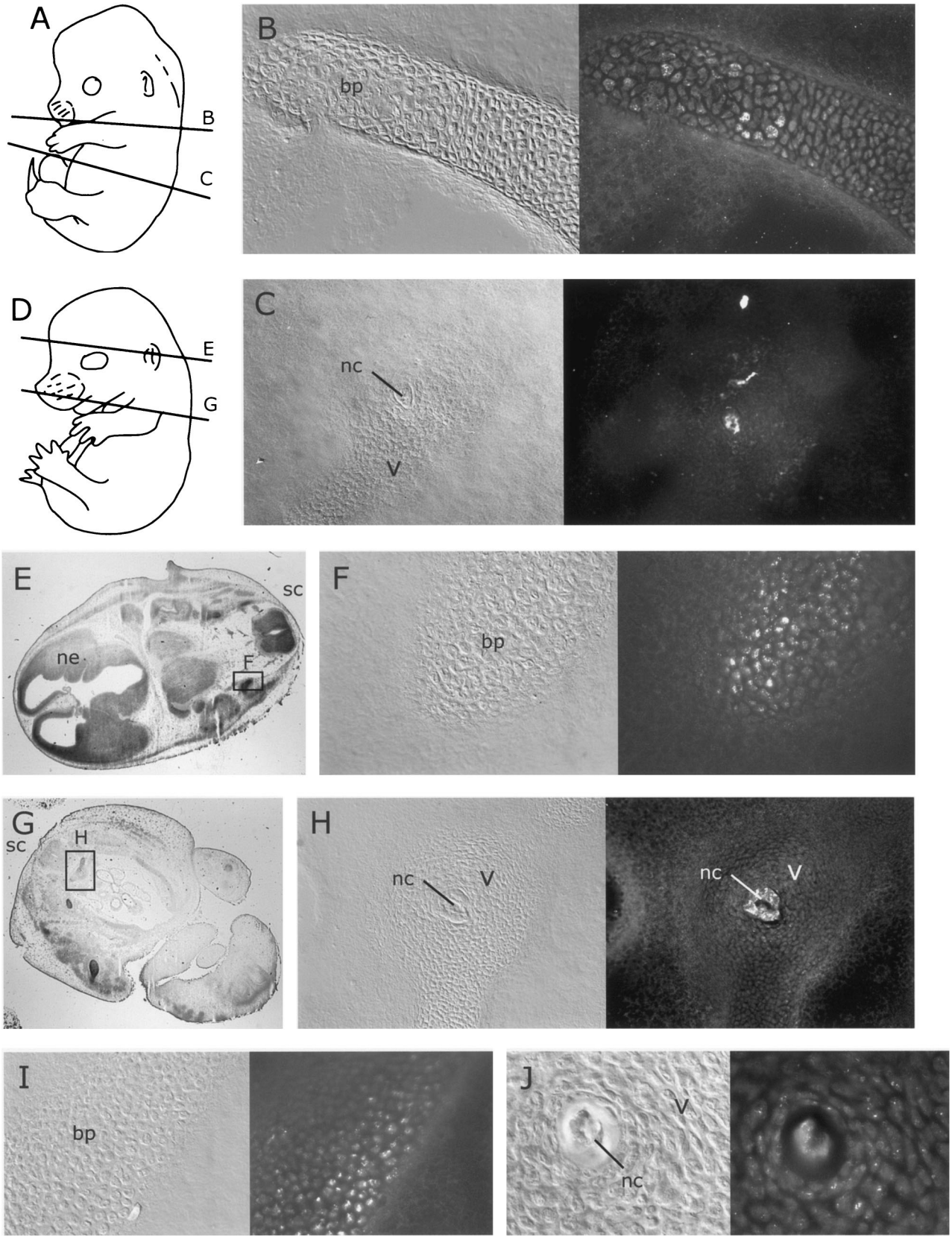

FIG. 3. Distribution of MVM coat proteins in embryos inoculated at 12.5 dpc after a further 24 or 48 h of gestation. For format, see the legend to Fig. 2. (A and D) Approximate planes of sections in panels B, C, E, and G. (B) MVMi coat protein distribution in forelimb bone primordium 24 h after inoculation. (C) MVMp coat protein in the notochord 24 h after inoculation. (E and G) Whole sections showing locations of field in panels F and H. (F and H) Distribution of MVMi coat proteins in bone primordia and notochord 48 h after inoculation. (I and J) Distribution of MVMp coat proteins in bone primordia and notochord 48 h after inoculation. bp, bone primordium; nc, notochord; ne, neuroepithelium; sc, spinal chord.

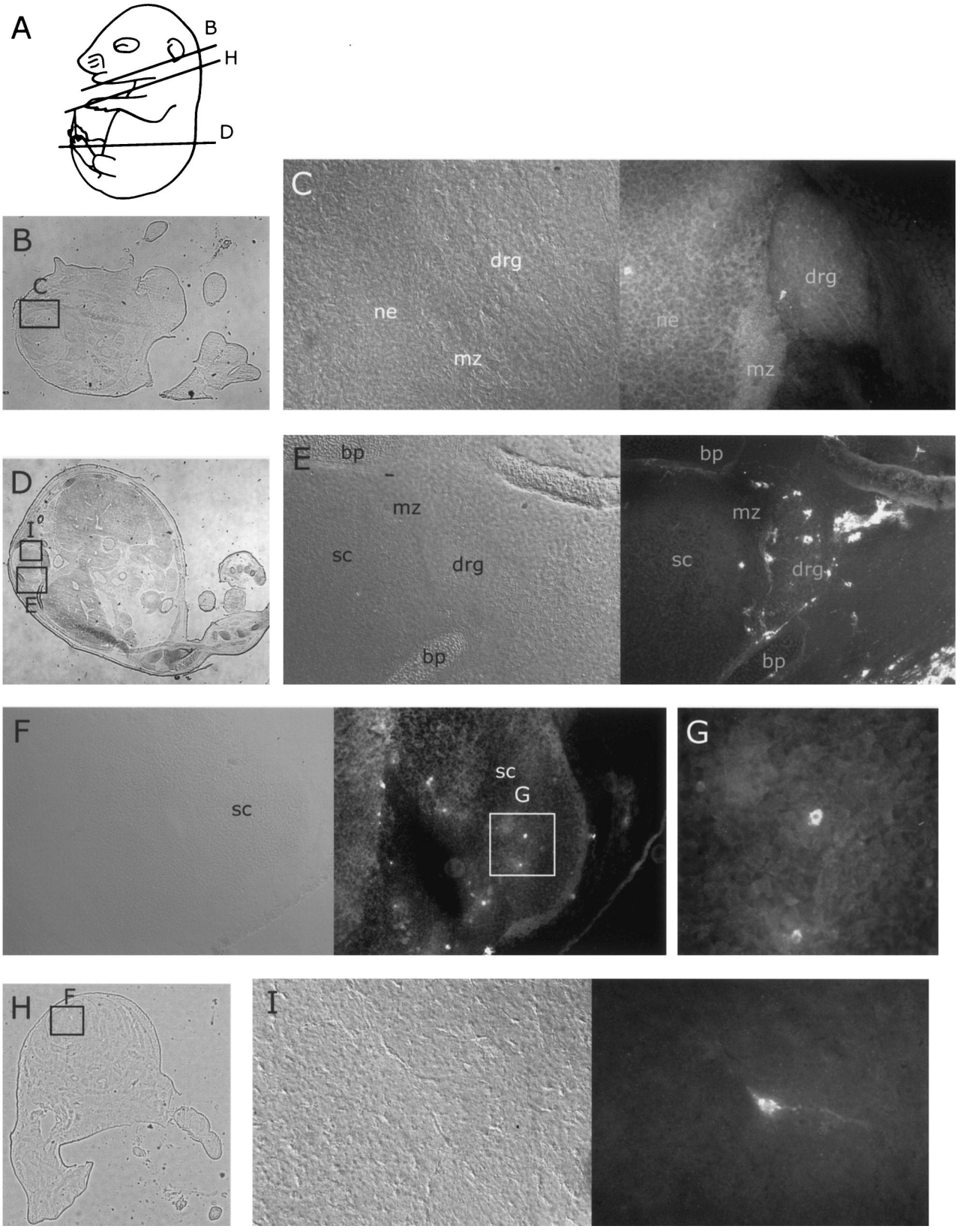

FIG. 4. Distribution of MVM coat proteins in neural tissues of embryos inoculated at 12.5 dpc after a further 96 h of gestation. For format, see the legend to Fig. 2. (A) Approximate planes of sections in panels B, D, and H. (B) Whole section showing location of field in panel C. (C and E) Embryonic dorsal root ganglia and parts of spinal chord 96 h after inoculation with MVMi (C) or MVMp (E), showing occasional immunoreactive cells in the ganglia. (H) Whole section showing field of view in panel F. (F, G, and I) Embryonic spinal chord 96 h after inoculation with MVMi (F and G) or MVMp (I), showing occasional immunoreactive cells in the spinal chord. bp, bone primordium; drg, dorsal root ganglion; mz, marginal zone; ne, neuroepithelium; sc, spinal chord.

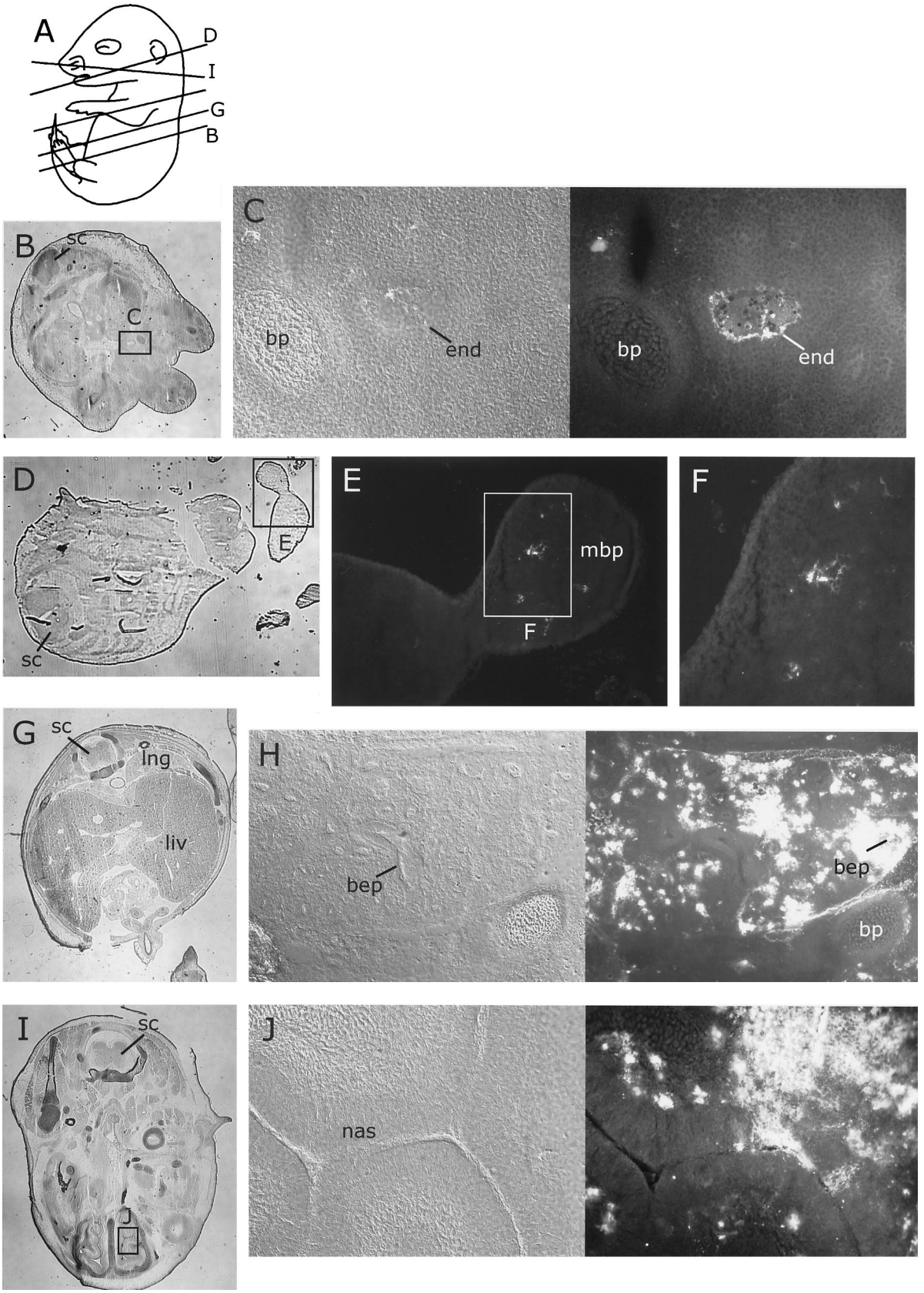

FIG. 5. Distribution of MVM coat proteins in nonneural tissues of embryos inoculated at 12.5 dpc after a further 96 h of gestation. For format, see the legend to Fig. 2. (A) Approximate planes of sections in panels B, D, G, and I. (B, D, G, and I) Whole sections showing fields of view in indicated figure panels. (B to F) Embryonic endothelium (C) and developing bone (E and F), showing distribution of MVMi coat proteins 96 h after inoculation. (G to J) Embryonic lung (H) and nasal (J) epithelium, showing large amounts of MVMp coat proteins 96 h after inoculation. bep, bronchi epithelium; bp, bone primordium; end, endothelium; liv, liver; lng, lung; mbp, mandible primordium; nas, nasal epithelium; sc, spinal chord.

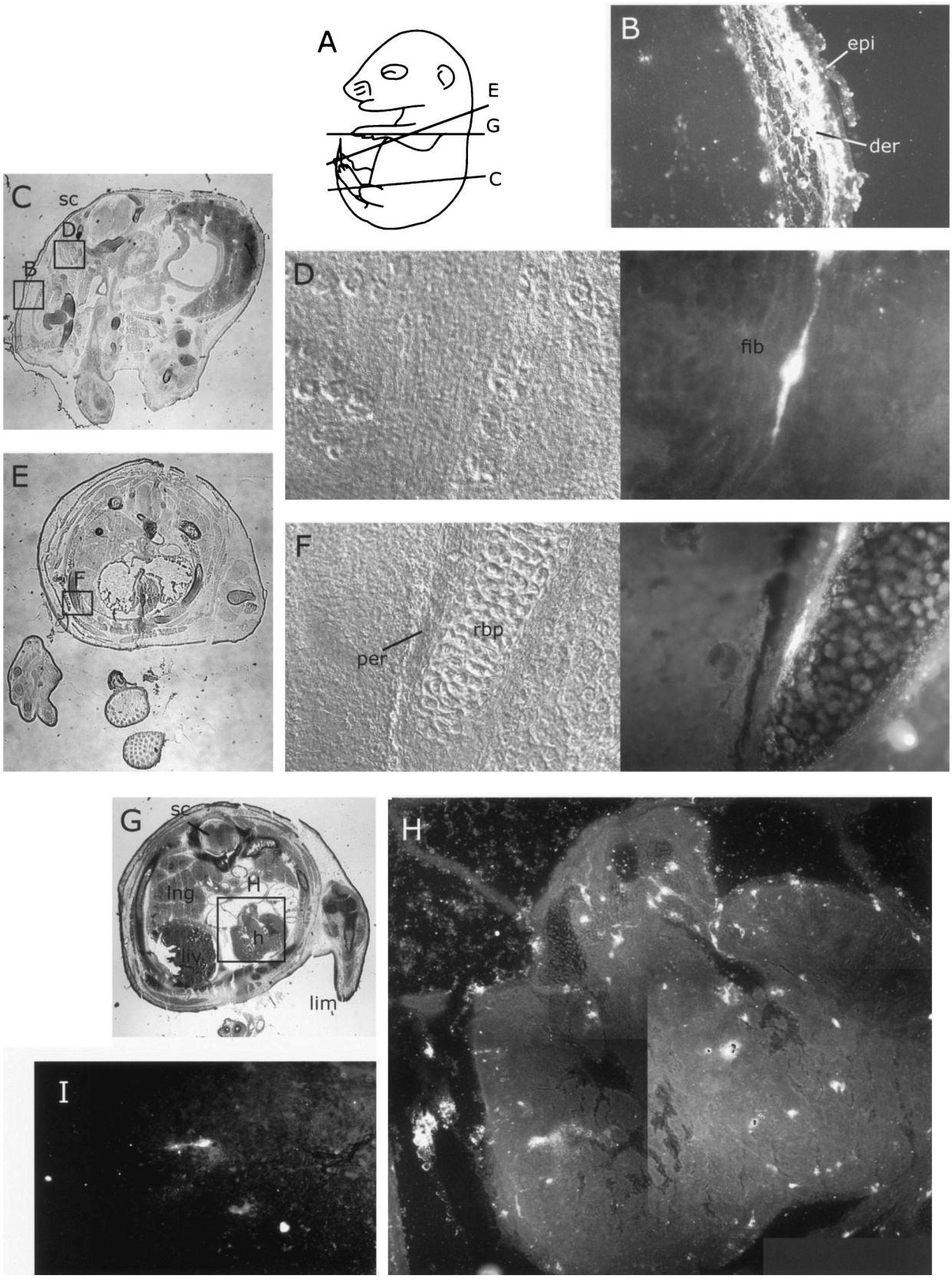

FIG. 6. Distribution of MVMp coat proteins in fibroblastic tissues of embryos inoculated at 12.5 dpc after a further 96 h of gestation. For format, see the legend to Fig. 2. (A) Approximate planes of sections in panels C, E, and G. (C, E, and G) Whole sections showing fields of view in indicated figure panels. (B) Section through developing skin, showing large amounts of MVMp in fibroblastic dermal layer but not in

and MVMi were observed in the developing nasal epithelium (Fig. 5J and data not shown). Some foci of infection were seen in the subarachnoid space, mainly in the area of the blood vessels passing anterior to the spinal cord. MVMi continued to infect some developing bone, notably the developing mandible and long bones of the limb (Fig. 5E).

DISCUSSION

Experimental data have shown that productive MVM infection requires a dividing cell population and depends upon the differentiation state of the potential host cell. Although the embryo consists largely of dividing cells in a range of differentiation states, the susceptibility of the developing embryo to infection by either virus strain has never been properly assessed. Also, our initial analysis of a transgenic MVM P4 promoter activity in the developing embryo suggested that the ability of the host cell to activate the promoter may constitute one of the host range determinants of MVM. By infecting the embryo, we could more directly compare the pattern of transgenic MVM P4 promoter activation with the pattern of MVM infection.

MVMi is more pathogenic than MVMp in the developing embryo. Early studies on the infection of neonates showed that MVMi administered oronasally mounted a lethal infection and was found disseminated throughout the animal, whereas similarly administered MVMp was innocuous. It was not clear whether this was due to an inability of MVMp to disseminate from the inoculation site (21) or to an inability to mount an infection in the host animal (4). The in utero infections described here show that both are capable of mounting an aggressive infection, disseminating to tissues throughout the embryo, and that both can kill the embryo. The kinetics of early infection are similar; between 24 and 48 h, both virus strains infected bone primordia at the same rate and to the same extent. At later times, MVMp spread rapidly to fibroblastic cells throughout the embryo, resulting in widespread infection and a high viral burden. In contrast, infection with MVMi remained restricted largely to the developing bone and later endothelium, with scattered infected cells in the CNS and a much lower viral burden. Despite the more restricted viral infection, MVMi was significantly more pathogenic, resulting in more and faster embryonic death than with MVMp. The developing embryo is quite resistant to tissue damage. Loss of function or structure often results in continued development and death at birth. The most critical exception is the embryonic cardiovascular system, where loss of function results in rapid embryonic death and resorption. It is most likely that the increased pathogenicity of MVMi compared to MVMp, despite the lower viral burden, is due to its observed infection of endothelium, as was proposed for MVMi-infected neonates (4). However, unlike infection in the neonates, where infection of the renal capillaries was judged the most likely cause of death, we did not observe any histological damage to infected endothelium anywhere in the embryo, and so cannot yet confirm the immediate cause of death.

Patterns of infection. Three distinct patterns of signal above background were observed in different embryonic tissues. (We exclude the strong signal at the injection site in the liver, which is certainly due to incoming virus.) In many tissues (bone, mesenchyme, endothelium, some epithelial tissues, and the developing placenta) strong immunoreactivity was observed over localized regions (foci) covering hundreds of cells, with extensive involvement of cells within the region (see, e.g., Fig. 5H). This pattern suggests a rapid and local production and spread of virus. The second pattern was occasional strongly positive cells in some tissue types (see, e.g., Fig. 4F). This pattern was typical of both MVMp and MVMi in the developing CNS and the dorsal root ganglia and perhaps of MVMp in the developing heart. Although not quantitative, the staining intensity in individual infected cells was similar to the staining intensity within the cells of infection foci, suggesting that the per-cell viral burden was similar. Such a pattern might be expected if the viral life cycle is partially or temporarily blocked in these cells, resulting in poor local cell-cell transmission of the virus but still resulting in the eventual accumulation of similar quantities of viral coat proteins in infected cells. Finally, an embryo-wide weak signal, which varied somewhat in strength in different tissues, was observed in the embryos infected at 9.5 dpc (see, e.g., Fig. 2I); this most probably represents an accumulation in the embryo of virus shed by the observed strong placental infection. The possibility that some cell types hosted productive infection but were not observed must also be considered. Since MVM infection rapidly kills some cultured cell types, perhaps some cells died before we observed their infection. We cannot exclude this possibility, but we can place a boundary on its frequency. Recent experiments in which we have injected other MVM variant viruses indicate that we are able to identify MVM-mediated cell killing in infection foci involving fewer than 50 cells (data not shown).

Expansion of the host range of MVMi and MVMp into overlapping sets of cell types. Some cell type tropisms observed in neonate or tissue culture studies were not observed in the embryos. Neither infection in the stomach (21) nor hematopoietic infections (4) (whether in the blood or liver) were seen in utero, although rare positive cells tentatively identified as lymphocytes were observed in MVMi-infected embryos. Some of this difference is perhaps due to the stages of embryonic development examined. The mature T-cell lineages known to be infected by MVMi appear late in development. The T-cell progenitors do not arrive in the thymus until between 12 and 14 dpc (12), and the *Notch1*-dependent T-cell lineage differentiation events are postnatal (30), whereas the latest embryonic stage we examined was 16.5 dpc.

The immunohistochemical data indicate that a number of tissue types in the developing embryo that had not been identified previously as MVM host cell types were capable of sup-

ectoderm-derived epidermal layer. (D) Section through mesenchymal tissue showing single intensely labeled fibroblast. (F) Section through developing bone showing MVMp coat proteins in fibroblast-derived periost. (H) Composite of heart section showing scattered distribution of intensely labeled putative fibroblast cells. (I) Single intensely labeled fibroblast in the heart myocardium. der, dermis; epi, epidermis; fib, fibroblast; lim, limb bud; liv, liver; lng, lung; per, periost; rbp, rib primordium; sc, spinal chord.

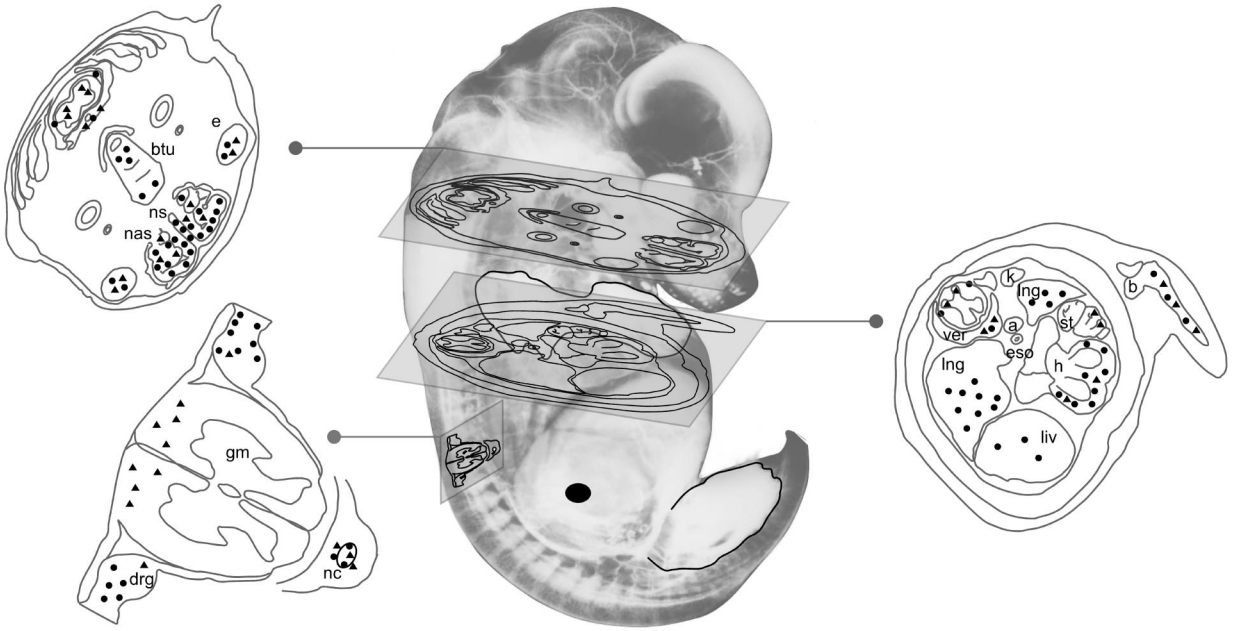

FIG. 7. Relative distribution of MVMp and MVMi infection following inoculation of the mouse embryo in utero. An image of an approximately 15.5-dpc mouse embryo in which the vasculature and peripheral nervous system has been highlighted is shown. The site of inoculation into the embryonic liver is indicated by a large filled circle. The fore- and hindlimbs of the right side of the embryo are outlined. Satellite diagrams of sections through the embryo are marked with symbols representing loci of MVMi infection (filled triangles) and MVMp infection (filled circles). The approximate placements of the diagrams within the embryo are indicated by the transecting planes. a, aorta; b, bone primordium; btu, base of tongue; drg, dorsal root ganglion; e, eye; eso, esophagus; gm, grey matter; h, heart; k, kidney; liv, liver; lng, lung; nas, nasal epithelium; nc, notochord; ns, nasal septum; st, stomach; ver, vertebrae.

porting productive MVM infection. Certainly the MVMi/MVMp reciprocal tropism observed in tissue culture (14, 15, 32, 38) and in neonate studies (4, 21) is still discernible in the embryo. MVMp showed extensive infection of fibroblasts, whereas MVMi infection was prominent in endothelium of blood vessels; however, both virus strains exhibited productive infection in bone primordia, notochord, CNS, and dorsal root ganglia (summarized in Fig. 7). This expansion of the host range and its overlap are not surprising. The embryo presents a richer supply of different populations of dividing cells in various differentiation states than either the neonate or the adult animal. With respect to the overlap, it has already been shown that cultured NB324K cells (simian virus 40-transformed human kidney cells) and TM4 cells (derived from mouse Sertoli cells) support lytic infection by both viruses (7, 16, 28).

The data also indicate a diverging host range in the developing bone. At 24 and 48 h after development, similar MVMi and MVMp infection was evident in bone primordia. After 96 h of further gestation, only MVMi infected bone; however MVMp was observed in the periost. The time interval when embryonic MVM infection was characterized is a very active one with respect to bone development. The axial and limb and jaw bone primordia result from mesenchymal condensation followed by differentiation into chondrocytes and then into hyperproliferative chondrocytes. This process begins at approximately 11.5 dpc, and the later process of differentiation into hyperproliferative chondrocytes continues throughout late embryogenesis. The chondrocytes lay down a cartilaginous model of the later bone. At approximately 14.0 dpc other mesenchymal cells of the periost differentiate into osteoblasts and invade these bone primordia. In contrast, the flat skull bones (calvaria) are produced by intramembranous ossification, a process which does not involve chondrocytes or a cartilaginous template (10, 42). Since we observe MVM infection in the bone primordia prior to the appearance of active osteoblasts and do not observe infection in the developing calvaria, the primary cell type infected by MVM in the developing bone is undoubtedly chondrocytes. The later infection of cells in the periost raises the possibility that early osteoblasts may also be susceptible to MVMp, but not MVMi, infection.

The MVMp infection of fibroblasts is interesting from a developmental viewpoint. The early embryonic mesenchyme that forms following gastrulation later gives rise to chondrocytes, osteoblasts, endothelium, adipocytes, smooth muscle, and fibroblasts. The differentiation mechanisms which give rise to all of these have been successfully studied at the molecular level, except for fibroblasts, which remain an ambiguous collection of later mesenchymal cells. There are very few fibroblast-specific markers (35). The MVMp infection of late-development fibroblasts, but not of the abundant early-development mesenchyme, confirms the existence of a so-far very poorly characterized developmental pathway.

The overall distribution of embryonic infection raises again the question of the determinants of susceptibility to the virus. Host cell components are important at all steps in the viral life cycle, but very few have been identified. The observation that strain-specific variation in host cell type maps to the viral capsid proteins certainly indicates that some unknown intracellular factors interact differentially with the viral coat pro-

teins. However, the role of other viral components in determining the host cell type range cannot be excluded. There are many other sequence variations between MVMi and MVMp, including three nucleotide changes in the P4 promoter and 15 amino acid changes in the NS proteins, which may not play a role in specifying the previously observed host range differences between the virus strains but which may be involved in specifying the more complete host range determined here. On the host side of the interaction, there are no obvious cell-type-specific variations in molecular components that could account for the differential response to the virus strains.

Infection versus transgenic P4 promoter activity. We have shown that a transgenic MVM P4 promoter exhibits a dynamic tissue- and stage-specific pattern of activation (9) (Fig. 1), and we have hypothesized that the ability of the host cell to activate the P4 promoter may constitute a host cell type determinant of MVM. An initial comparison of the transgenic promoter activity in the embryo or adult and the host cell type range in neonate mice was consistent with the suggestion but was weakened by the disparate developmental stages involved. A closer comparison of the patterns of infection and transgenic P4 activity is made possible by this in utero infection study. Indeed, the comparison between P4 activity (9) and VP expression may be incomplete, because P4 activity by itself does not necessarily assure capsid formation. We are currently studying early events (NS1 and NS2 production) in embryonic infections.

Numerous cell types that were shown to activate the transgenic promoter were also susceptible to either MVMi or MVMp infection (Table 2), including the previously uncharacterized host cells of the bone primordia, the notochord, and the dorsal root ganglia. Embryos at 9.5 dpc, which did not activate the P4 promoter, also failed to develop clear infections, although they contain cell types, such as neuroepithelium, endothelium, and mesenchyme, which would later both exhibit activation of the P4 promoter and support MVM infection. This finding is consistent with the observation that undifferentiated embryonic carcinoma cells in culture were resistant to infection, whereas differentiated derivatives were sensitive (27).

Since there are other host range-determining interactions between the virus and potential host cell, it is to be expected that some cell types will express the promoter but remain resistant to infection. Certainly in the embryo, the developing CNS activated the transgenic P4 promoter relatively strongly (Fig. 1). Nevertheless, infection in the embryonic CNS was restricted to scattered cells. Similarly, transgene activation was observed in the cardiomyocytes, but the MVM infection that we observed in the heart is likely fibroblastic or, at most, some scattered cardiomyocytes. We observed one tissue, the embryonic bronchus, in which the transgenic P4 promoter was not active yet was susceptible to infection. There is a possibility that this discrepancy is due to the difference in time of analysis, since the bronchi of the adult lung were shown to express the transgene whereas the embryonic bronchi were established to be negative at 13.5 dpc (9). Although the transgene expression studies were done with BALB/c mice and the in utero infections were done with CD-1 mice, we do not think that mouse strain differences are responsible for the observed discrepancy. The transgene-bearing BALB/c mice were crossed with CD-1

TABLE 2. Tissue distribution of MVM following in utero infection at 12.5 dpc and subsequent gestation compared to transgenic P4 promoter activity

Tissue	Postinjection incubation time (h)	Extent of tissue-specific infection with[a]:	
		MVMp	MVMi
Chondrocyte (bone primordium)[b]	24	++	++
	48	++	++
	96	++	++
Notochord[b]	24	++	++
	48	++	++
	96	+	+
Cardiomyocyte[b]	24	+	+
	48	+	+
	96	+++	+
Endothelium[b]	24	−	−
	48	−	+
	96	−	++
Fibroblast[b]-mesenchyme	24	−	−
	48	+	−
	96	+++	−
Dermis[b]	24	−	−
	48	−	−
	96	+++	−
Smooth muscle[b]	24	−	−
	48	−	−
	96	+	−
Neuroectoderm[b]	24	−	−
	48	−	+
	96	++	++
Kidney	24	−	−
	48	−	−
	96	−	−
Epidermis	24	−	−
	48	−	−
	96	−	−
Nasal epithelium[b]	24	−	−
	48	−	+
	96	+++	++
Eye (lens + retina)[b]	24	−	−
	48	−	−
	96	+	+
Dorsal root ganglia[b]	24	−	−
	48	+	+
	96	+	++
Hepatocytes[b]	24	−	−
	48	+	+
	96	+	−
Lung epithelium	24	−	−
	48	−	−
	96	+++	+
Gut epithelium[b]	24	−	−
	48	−	−
	96	+	−
Pancreatic epithelium	24	−	−
	48	−	−
	96	−	−

[a] −, no infection observed; +, rare individual cells or foci observed (see, e.g., Fig. 4F); ++, more extensive infection foci observed (see, e.g., Fig. 3B); +++, extensive infection often involving large portions of the full thickness of the target tissue (see, e.g., Fig. 5J).

[b] Tissue in which the P4 promoter was active at 12.5 and 13.5 dpc (9).

mice, and staining in the first- and second-generation embryos was the same as that in the BALB/c mice (data not shown). The transgene was irreversibly and completely shut off in subsequent CD-1 generations. We were unable to regain expression by backcrossing to BALB/c mice, suggesting that the observed attenuation was due to strain-specific transgene inactivation, a familiar phenomenon, rather than to strain-specific variations in promoter activity (C. Davis and J. Tal, unpublished data).

The observed correlation between infected cell type and expression of the transgene in the embryo strengthens the hypothesis that activation of the P4 promoter by the host cell is a host range determinant. Further experiments to address the hypothesis more rigorously are in progress.

ACKNOWLEDGMENTS

This work was supported by grants from the Israel-USA Binational Science Foundation (to J.T.) and from the Israel Science Foundation (to C.D. and J.T.).

We thank Peter Tatersall for the original MVMi and MVMp stocks and Michal Mincberg for virus preparations.

REFERENCES

1. **Ball-Goodrich, L. J., R. D. Moir, and P. Tattersall.** 1991. Parvoviral target cell specificity: acquisition of fibrotropism by a mutant of the lymphotropic strain of minute virus of mice involves multiple amino acid substitutions within the capsid. Virology **184:**175–186.
2. **Bolt, D. M., H. Hani, E. Muller, and A. S. Waldvogel.** 1997. Non-suppurative myocarditis in piglets associated with porcine parvovirus infection. J. Comp. Pathol. **117:**107–118.
3. **Bonnard, G. D., E. K. Manders, D. A. Campbell, Jr., R. B. Herberman, and M. J. Collins, Jr.** 1976. Immunosuppressive activity of a subline of the mouse EL-4 lymphoma. Evidence for minute virus of mice causing the inhibition. J. Exp. Med. **143:**187–205.
4. **Brownstein, D. G., A. L. Smith, R. O. Jacoby, E. A. Johnson, G. Hansen, and P. Tattersall.** 1991. Pathogenesis of infection with a virulent allotropic variant of minute virus of mice and regulation by host genotype. Lab. Investig. **65:**357–364.
5. **Brownstein, D. G., A. L. Smith, E. A. Johnson, D. J. Pintel, L. K. Naeger, and P. Tattersall.** 1992. The pathogenesis of infection with minute virus of mice depends on expression of the small nonstructural protein NS2 and on the genotype of the allotropic determinants VP1 and VP2. J. Virol. **66:**3118–3124.
6. **Cater, J. E., and D. J. Pintel.** 1992. The small non-structural protein NS2 of the autonomous parvovirus minute virus of mice is required for virus growth in murine cells. J. Gen. Virol. **73:**1839–1843.
7. **Clemens, K. E., and D. Pintel.** 1987. Minute virus of mice (MVM) mRNAs predominantly polyadenylate at a single site. Virology **160:**511–514.
8. **Crawford, L. V.** 1966. A minute virus of mice. Virology **29:**605–612.
9. **Davis, C., N. Segev-Amzaleg, I. Rotem, M. Mincberg, N. Amir, S. Sivan, I. Gitelman, and J. Tal.** 2003. The P4 promoter of the parvovirus minute virus of mice is developmentally regulated in transgenic P4-LacZ mice. Virology **306:**268–279.
10. **de Crombrugghe, B., V. Lefebvre, and K. Nakashima.** 2001. Regulatory mechanisms in the pathways of cartilage and bone formation. Curr. Opin. Cell Biol. **13:**721–727.
11. **Deleu, L., A. Pujol, S. Faisst, and J. Rommelaere.** 1999. Activation of promoter P4 of the autonomous parvovirus minute virus of mice at early S phase is required for productive infection. J. Virol. **73:**3877–3885.
12. **Douagi, I., I. Andre, J. C. Ferraz, and A. Cumano.** 2000. Characterization of T cell precursor activity in the murine fetal thymus: evidence for an input of T cell precursors between days 12 and 14 of gestation. Eur. J. Immunol. **30:**2201–2210.
13. **Durham, P. J., A. Lax, and R. H. Johnson.** 1985. Pathological and virological studies of experimental parvoviral enteritis in calves. Res. Vet. Sci. **38:**209–219.
14. **Gardiner, E. M., and P. Tattersall.** 1988. Evidence that developmentally regulated control of gene expression by a parvoviral allotropic determinant is particle mediated. J. Virol. **62:**1713–1722.
15. **Gardiner, E. M., and P. Tattersall.** 1988. Mapping of the fibrotropic and lymphotropic host range determinants of the parvovirus minute virus of mice. J. Virol. **62:**2605–2613.
16. **Guetta, E., D. Ron, and J. Tal.** 1986. Development-dependent replication of minute virus of mice in differentiated mouse testicular cell lines. J. Gen. Virol. **67:**2549–2554.
17. **Hueffer, K., and C. R. Parrish.** 2003. Parvovirus host range, cell tropism and evolution. Curr. Opin. Microbiol. **6:**392–398.

17a. **Itah, R., I. Gitelman, Y. Tal, and C. Davis.** 2004. A protocol for viral inoculation of mouse embryos in utero. J. Virol. Methods **120:**1–8.

18. **Jacoby, R. O., L. J. Ball-Goodrich, D. G. Besselsen, M. D. McKisic, L. K. Riley, and A. L. Smith.** 1996. Rodent parvovirus infections. Lab. Anim. Sci. **46:**370–380.
19. **Kaufman, M. H.** 1992. The atlas of mouse development. Academic Press, San Diego, Calif.
20. **Kilham, L., and G. Margolis.** 1971. Fetal infections of hamsters, rats, and mice induced with the minute virus of mice (MVM). Teratology **4:**43–61.
21. **Kimsey, P. B., H. D. Engers, B. Hirt, and C. V. Jongeneel.** 1986. Pathogenicity of fibroblast- and lymphocyte-specific variants of minute virus of mice. J. Virol. **59:**8–13.
22. **Linser, P., H. Bruning, and R. W. Armentrout.** 1977. Specific binding sites for a parvovirus, minute virus of mice, on cultured mouse cells. J. Virol. **24:**211–221.
23. **Lukashov, V. V., and J. Goudsmit.** 2001. Evolutionary relationships among parvoviruses: virus-host coevolution among autonomous primate parvoviruses and links between adeno-associated and avian parvoviruses. J. Virol. **75:**2729–2740.
24. **Maxwell, I. H., A. L. Spitzer, F. Maxwell, and D. J. Pintel.** 1995. The capsid determinant of fibrotropism for the MVMp strain of minute virus of mice functions via VP2 and not VP1. J. Virol. **69:**5829–5832.
25. **McMaster, G. K., P. Beard, H. D. Engers, and B. Hirt.** 1981. Characterization of an immunosuppressive parvovirus related to the minute virus of mice. J. Virol. **38:**317–326.
26. **Mengeling, W. L., K. M. Lager, J. K. Zimmerman, N. Samarikermani, and G. W. Beran.** 1991. A current assessment of the role of porcine parvovirus as a cause of fetal porcine death. J. Vet. Diagn. Investig. **3:**33–35.
27. **Miller, R. A., D. C. Ward, and F. H. Ruddle.** 1977. Embryonal carcinoma cells (and their somatic cell hybrids) are resistant to infection by the murine parvovirus MVM, which does infect other teratocarcinoma-derived cell lines. J. Cell Physiol. **91:**393–401.
28. **Naeger, L. K., J. Cater, and D. J. Pintel.** 1990. The small nonstructural protein (NS2) of the parvovirus minute virus of mice is required for efficient DNA replication and infectious virus production in a cell-type-specific manner. J. Virol. **64:**6166–6175.
29. **Parrish, C. R.** 1995. Pathogenesis of feline panleukopenia virus and canine parvovirus. Baillieres Clin. Haematol. **8:**57–71.
30. **Radtke, F., A. Wilson, G. Stark, M. Bauer, J. van Meerwijk, H. R. MacDonald, and M. Aguet.** 1999. Deficient T cell fate specification in mice with an induced inactivation of Notch1. Immunity **10:**547–558.
31. **Ramirez, J. C., A. Fairen, and J. M. Almendral.** 1996. Parvovirus minute virus of mice strain i multiplication and pathogenesis in the newborn mouse brain are restricted to proliferative areas and to migratory cerebellar young neurons. J. Virol. **70:**8109–8116.
32. **Ron, D., P. Tattersall, and J. Tal.** 1984. Formation of a host range mutant of the lymphotropic strain of minute virus of mice during persistent infection in mouse L cells. J. Virol. **52:**63–69.
33. **Rubio, M. P., S. Guerra, and J. M. Almendral.** 2001. Genome replication and postencapsidation functions mapping to the nonstructural gene restrict the host range of a murine parvovirus in human cells. J. Virol. **75:**11573–11582.
34. **Spalholz, B. A., and P. Tattersall.** 1983. Interaction of minute virus of mice with differentiated cells: strain-dependent target cell specificity is mediated by intracellular factors. J. Virol. **46:**937–943.
35. **Strutz, F., H. Okada, C. W. Lo, T. Danoff, R. L. Carone, J. E. Tomaszewski, and E. G. Neilson.** 1995. Identification and characterization of a fibroblast marker: FSP1. J. Cell Biol. **130:**393–405.
36. **Tattersall, P.** 1972. Replication of the parvovirus MVM. I. Dependence of virus multiplication and plaque formation on cell growth. J. Virol. **10:**586–590.
37. **Tattersall, P.** 1978. Susceptibility to minute virus of mice as a function of host-cell differentiation, p. 131–149. *In* D. C. Ward and P. Tattersall (ed.), Replication of mammalian parvoviruses. Cold Spring Harbor Laboratory, Cold Spring Harbor, N.Y.
38. **Tattersall, P., and J. Bratton.** 1983. Reciprocal productive and restrictive virus-cell interactions of immunosuppressive and prototype strains of minute virus of mice. J. Virol. **46:**944–955.
39. **Tattersall, P., and D. C. Ward.** 1978. The parvoviruses—an introduction, p. 3–12. *In* D. C. Ward and P. Tattersall (ed.), Replication of mammalian parvoviruses. Cold Spring Harbor Laboratory Press, Cold Spring Harbor, N.Y.
40. **Toolan, H. W.** 1978. Maternal role in susceptibility of embryonic and newborn hamsters to H-1 parvovirus, p. 161–178. *In* D. C. Ward and P. Tattersall (ed.), Replication of mammalian parvoviruses. Cold Spring Harbor Laboratory Press, Cold Spring Harbor, N.Y.
41. **Truyen, U., and C. R. Parrish.** 2000. Epidemiology and pathology of autonomous parvoviruses. Contrib. Microbiol. **4:**149–162.
42. **Wagner, E. F., and G. Karsenty.** 2001. Genetic control of skeletal development. Curr. Opin. Genet. Dev. **11:**527–532.
43. **Wolter, S., R. Richards, and R. W. Armentrout.** 1980. Cell cycle-dependent replication of the DNA of minute virus of mice, a parvovirus. Biochim. Biophys. Acta **607:**420–431.